36th EPS Conference on Plasma Phys. Sofia, June 29 - July 3, 2009 ECA Vol.**33E**, P-4.210 (2009)

Heat and Particle Transport Experiments in Tore Supra and HL-2A with ECRH and SMBI

X.L. Zou, S.D. Song, G. Giruzzi, C. Honore[1], J.L. Ségui, D. Elbeze, F. Clairet, R. Sabot, J. Bucalossi, P. Hennequin[1], F. Bouquey, M. Lennholm, R. Magne, E. Traisnel and Tore Supra team
CEA, IRFM, F-13108 Saint-Paul-lez-Durance, France
1) LPTP, Ecole Polytechnique, 91128 Palaiseau, France

W.W. Xiao, X.T. Ding, Y. Shen, J. Rao, J. Zhou, L.H. Yao, B.B. Feng, C.Y. Chen, X.M. Song, Y. Zhou, L.C. Li, D.L. Yu, Z.T. Liu, B.S. Yuan, H.J. Sun, X.Q. Ji, Y.D. Gao, W. Chen, Y.G. Li, L.W. Yan, Q.W. Yang, Yi Liu, J.Q. Dong, X.R. Duan, C.H. Pan, Yong Liu and HL-2A team
Southwestern Institute of Physics, P.O. Box 432, Chengdu, China

1) ECRH modulation experiments

Experiments with ECRH have been recently performed in Tore Supra and HL-2A to investigate the heat and particle transport. Strong inward heat transport has been observed in Tore Supra in an off-axis ECRH experiment (half radius ECRH deposition) for low density ($\bar{n}_e \approx 1.5\times10^{19}\,m^{-3}$) (Fig.1), where a hot pulse (red) propagates from the mid-radius to the central region. Fig.2 shows the time evolution of the temperature heating profile with ECRH. The heat starts to increase at the ECRH deposition, then extends to the central region by diffusion and convection, and at the final stage the temperature at the centre is much higher than that at the ECRH deposition. This is often considered as a strong signature for the heat pinch. Fig.3 shows the FFT analysis of the temperature modulated by ECRH at 1 Hz. The solid lines represent the simulation with an analytical transport model [1]. Good agreement has been found between the simulation and experimental points for harmonics from 1 to 11. The transport coefficients used in this simulation is shown in Fig.4. A pinch velocity of order of 2-3*m/s* has been found in the plasma central region inside the ECRH deposition layer. These results are very similar to that observed in the past on DIII-D [2] and RTP [3]. Analogous results have been obtained on HL-2A in the ECRH modulation experiments. Note that for higher density $\bar{n}_e \approx 3.5\times10^{19}\,m^{-3}$ this inward heat transport is strongly reduced.

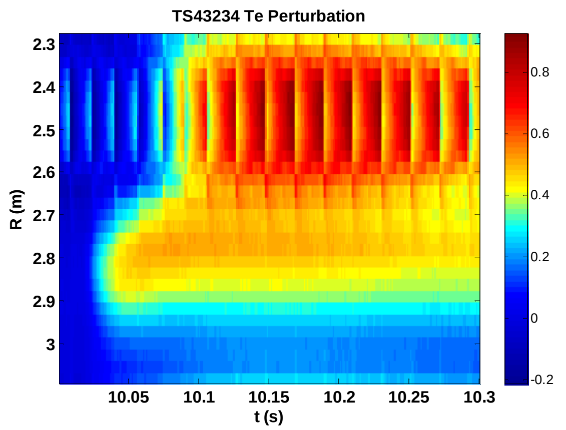

Fig.1 2D image of the temperature variation during ECRH.

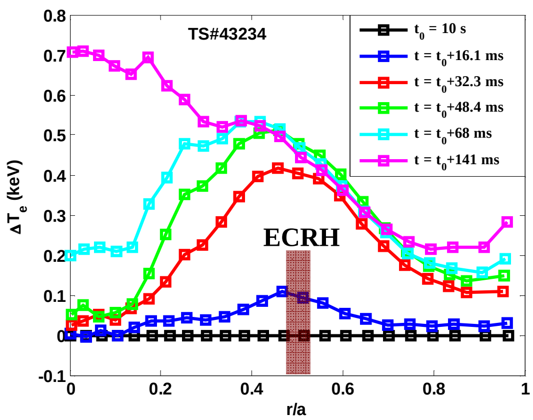

Fig.2 Time evolution of the temperature variation profile during ECRH.

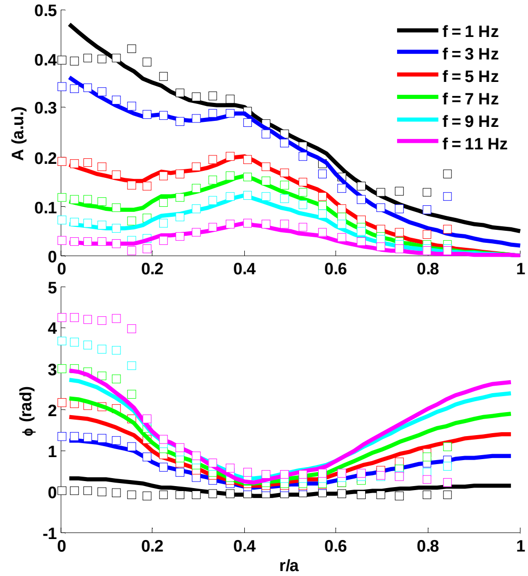

Fig.3 Amplitude and phase of the harmonics 1, 3, 5, 7, 9, 11 of the Fourier transform of the modulated temperature. Solid lines for simulation.

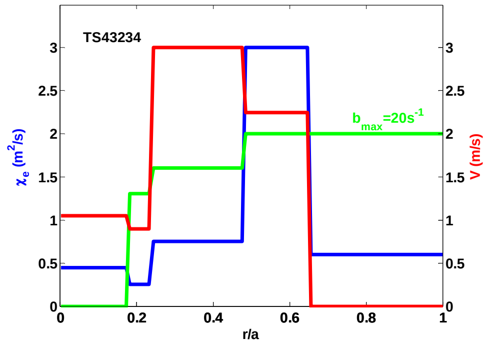

Fig.4 Radial profile of the diffusivity χ_e, the damping time ($\tau_D = 1/b$), and pinch velocity V used for simulation in the figure 3.

In addition to the pinch effect, a jump in the heat diffusivity has been observed at the ECRH deposition (Fig.4) as on ASDEX-U [4]. And at the same position, a jump in the particle diffusivity has also been observed using density modulation analysis. These observations suggest that ECRH creates an ITB on both heat and particle transport at its deposition layer.

2) SMBI modulation experiments

Edge cooling driving central heating (commonly called non local transport, NLT) has been observed in experiments performed with SMBI on both Tore Supra and HL-2A for ohmic plasmas. Fig.5 illustrates the strong central heating (>10%) due to SMBI observed in HL-2A. Fig.6 displays the 2D image of the temperature perturbation during SMBI in Tore Supra. From this figure, a very slow propagation of a cold pulse (blue) from the edge to the plasma centre is clearly observed, but the hot pulse in the central region is formed before the cold pulse reaches this region. As observed in the previous experiments with pellet [5], the temperature perturbation inversion zone is located outside of the *q*=1 surface, and it exists a threshold in density for the observation of this phenomenon (edge cooling driving central heating).

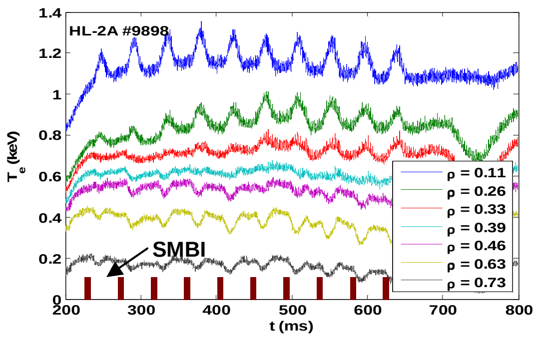

Fig.5 Time evolution of the temperature during the SMBI modulation in HL-2A.

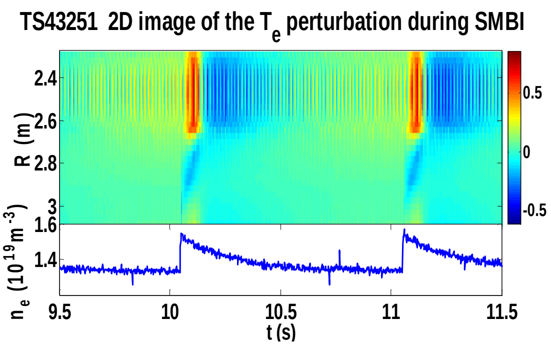

Fig6. 2D image of the temperature variation during SMB in Tore Supra.

Fig.7 shows the amplitude and phase of the Fourier transform of the temperature modulated by SMBI for two Tore Supra discharges, one for low density $\bar{n}_e \approx 1.4\times10^{19} m^{-3}$ and with NLT (TS#41628) , and another one for high density $\bar{n}_e \approx 2.9\times10^{19} m^{-3}$ without NLT (TS#41632). For these discharges, the magnetic field is $B_0 = 3.47T$, the plasma current is $I_p = 1.0MA$, the plasma major radius is $R = 2.38m$, and the plasma minor radius is $a = 0.72m$. In this figure, we can observe that the phase, which depends essentially the diffusivity, is nearly the same for the two cases in the region between the source (edge) and the temperature perturbation inversion zone (grey), but inside the latter, the phase bifurcates. It has been found by using analytical transport model that the heat diffusivity and the heat pinch velocity in this zone , which is illustrated by grey colour in the figure, are respectively $\chi_e = 0.23m^2/s$, $V^H = 1.4m/s$ for the NLT case, and $\chi_e = 1.28m^2/s$ and $V^H = 2.7m/s$ for the no NLT case. Thus a strong heat transport reduction has been observed in the temperature perturbation inversion zone for the NLT case.

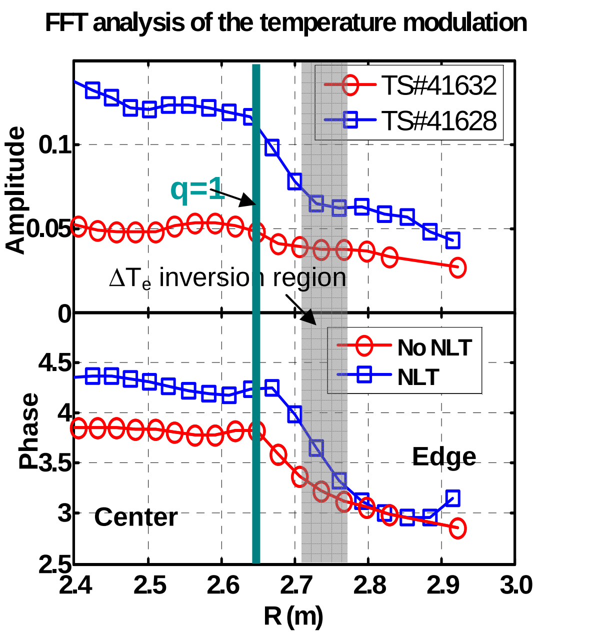

Fig.7 Amplitude and phase of the Fourier transform of the temperature during SMBI modulation with (TS#41628) and without NLT (TS#41632).

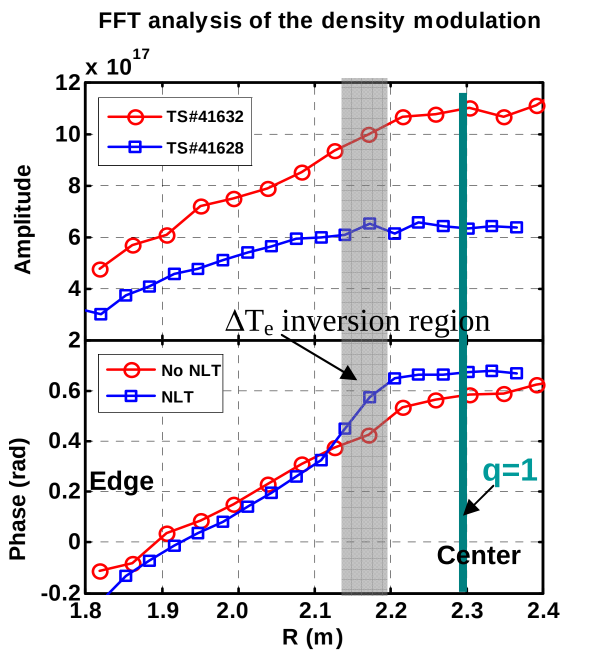

Fig.8 Amplitude and phase of the Fourier transform of the density during SMBI modulation with (TS#41628) and without NLT (TS#41632).

Fig.8 shows the results of the FFT analysis of the density modulation generated by SMBI. Note that the density is measured by an X mode reflectometer, which probes the high magnetic field side. Thus the measurement region for the density is from R=1.8m to R=2.4 m. In Fig.8 the corresponding temperature inversion zone, illustrated by the grey colour, lies between R=2.1m and R=2.2m. As for the temperature, similar results have been observed for the density. The phase is nearly the same in the region between the edge and the temperature perturbation inversion zone, where the particle diffusivity $D = 1.5m^2/s$ and the particle pinch $V^P = 5.5m/s$ for TS#41632 (no NLT), and $D = 1.3m^2/s$, $V^P = 3.5m/s$ for TS#41628 (NLT). Inside the temperature perturbation inversion zone, the phase bifurcates with respectively, $D = 1.1m^2/s$, $V^P = 1.8m/s$ for the no NLT case, $D = 0.4m^2/s$, $V^P = 0.4m/s$ for the NLT case. As for the heat, the particle transport is strongly reduced inside the temperature perturbation inversion zone. The temperature and density modulation analysis show the presence of ITBs on both heat and particle transport inside the temperature perturbation inversion zone during SMBI. In the ECRH phase, the inversion zone is shifted outwards with respect to the ECRH deposition.

In Tore Supra the turbulence rotation velocity perpendicular to the magnetic field is measured by the Doppler reflectometry. Fig.9 displays the turbulence perpendicular rotation velocity before (square) and after (circle) the SMBI for the discharge #41632 where no NLT is observed during SMBI. There is no significant change for the turbulence rotation velocity profile before and after SMBI. Fig.10 displays the turbulence perpendicular rotation velocity before (square) and after (circle) the SMBI for the discharge #41628 where NLT is observed during SMBI. In this figure two differences should be emphasised compared to Fig.9: the value of the turbulence rotation velocity is close to zero in the plasma core (r/a<0.8) before SMBI; significant change is clearly observed now for the turbulence rotation velocity profile before and after SMBI, and this velocity changes sign at the temperature perturbation inversion zone ($r/a \approx 0.4-0.5$). The time to obtain a velocity profile is about 5*ms*. We can imagine in the NLT case that the SMBI generates firstly a plasma rotation change at the temperature perturbation inversion region, where the plasma reaction time for the rotation can be much shorter than the diffusion time, because the molecular beam velocity is supersonic before ionization. Then this rotation shear is high enough to suppress the turbulence in this region, and leads to the ITB formation. Finally this ITB can be responsible for the central heating. Simulation with the ITB assumption can reproduce qualitatively the experimental observation. In this interpretation the heat transport is local.

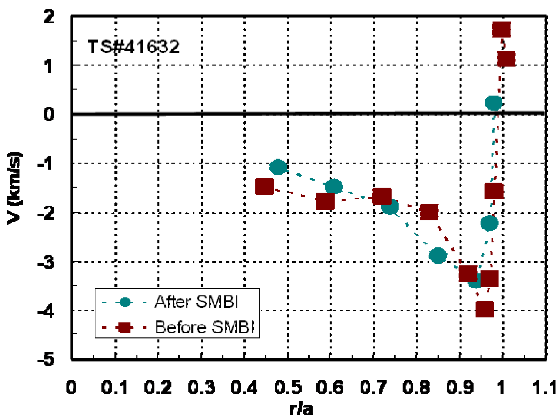

Fig. 9 Turbulence perpendicular rotation velocity before (red) and after (blue) the SMBI for the discharge #41632. No central heating has been observed during SMBI.

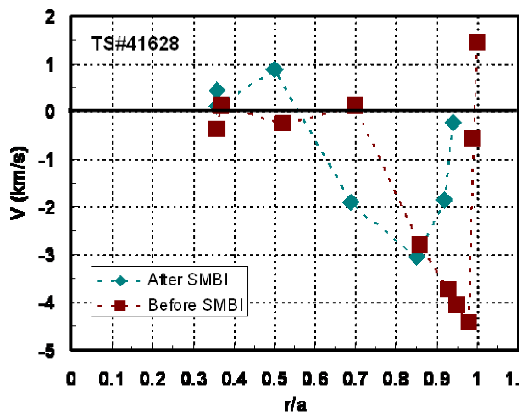

Fig. 10 Turbulence perpendicular rotation velocity before (red) and after (blue) the SMBI for the discharge #41628. A central heating has been observed during SMBI.

[1] S.P. Eury, E. Harauchamps, X.L. Zou, G. Giruzzi, Phys. Plasmas **12**, 102511 (2005)

[2] C. Petty, T.C. Luce, Nucl. Fusion **34**, 121 (1994).

[3] P. Mantica, G. Gorini, G.M.D. Hogeweij, N.J. Lopes Cardozo, A.M.R. Schilham, Phys. Rev. Lett. **85**, 4534 (2000).

[4] F. Ryter, F. Leuterer, G. Pereverzev, H.U. Fahrbach, J. Stober, W. Suttrop, and ASDEX Upgrade TEAM, Phys. Rev. Lett. **86**, 2325 (2001).

[5] X.L. Zou, A. Geraud, P. Gomez *et al.*, Plasma Phys. Control. Fusion **42**, 1067 (2000).